International Journal of Minerals, Metallurgy and Materials
Volume 18, Number 6, Dec 2011, Page 646
DOI: 10.1007/s12613-011-0490-1

Dissolution of Al_2TiO_5 inclusions in $CaO\text{-}SiO_2\text{-}Al_2O_3$ slags at 1823 K

De-yong Wang[1)], *Jun Liu*[1)], *Mao-fa Jiang*[1)], *Fumitaka Tsukihashi*[2)], *and Hiroyuki Matsuura*[2)]

1) School of Materials and Metallurgy, Northeastern University, Shenyang 110004, China

2) Department of Advanced Materials Science, Graduate School of Frontier Sciences, Tokyo University, Chiba 277-8561, Japan

(Received: 5 January 2011; revised: 31 March 2011; accepted: 7 April 2011)

Abstract: Al-Ti-O inclusions always clog submerged nozzles in Ti-bearing Al-killed steel. A typical synthesized Al_2TiO_5 inclusion was immersed in a $CaO\text{-}SiO_2\text{-}Al_2O_3$ molten slag for different durations at 1823 K. The Al_2TiO_5 dissolution paths and mechanism were revealed by scanning electron microscopy (SEM) and energy dispersive spectroscopy (EDS). Decreased amounts of Ti and Al and increased amounts of Si and Ca at the dissolution boundary prove that inclusion dissolution and slag penetration simultaneously occur. SiO_2 diffuses or penetrates the inclusion more quickly than CaO, as indicated by the $w(CaO)/w(SiO_2)$ value in the reaction region. A liquid product (containing 0.7-1.2 $w(CaO)/w(SiO_2)$, 15wt%-20wt% Al_2O_3, and 5wt%-15wt% TiO_2) forms on the inclusion surface when Al_2TiO_5 is dissolved in the slag. Al_2TiO_5 initially dissolves faster than the diffusion rate of the liquid product toward the bulk slag. With increasing reaction time, the boundary reaches its largest distance, the Al_2TiO_5 dissolution rate equals the liquid product diffusion rate, and the dissolution process remains stable until the inclusion is completely dissolved.

Keywords: steelmaking; aluminium titante; molten slag; inclusions; dissolution

[*This work was financially supported by the National Natural Science Foundation of China (No.50904017).*]

1. Introduction

Titanium (Ti) alloys are important for improving the quality of steel products. In low-alloy steel, Ti combines carbon (C) and/or nitrogen (N) to form stable compounds, such as TiN, TiC, or Ti(C,N). These compounds precipitating on the grain boundary, prevent the growth rate of austenite grains during the process of heating and rolling, and restrain austenite recovery and recrystallization [1-3]. They improve the intensity and toughness of steels, as well as guarantee its machinability and weldability. However, for Ti-bearing steels, particularly those containing aluminium (Al), liquid steel presents poor castability. Additionally, submerged nozzles tend to be clogged severely.

Al-Ti-O inclusions in liquid steel have been reported to increase the tendency of submerged nozzles clogging. Kawashima *et al*. [4] reported that the frequent of nozzle clogging during the casting of Fe-Al-Ti alloys is attributed to Al-Ti-O oxide formed by reoxidation during tapping. Basu *et al*. [5] reported that reoxidation is detrimental to the castability of all Al-killed steels; it becomes worse in Ti-bearing Al-killed steels. This is primarily because of the formation of Ti-bearing alumina inclusions ($Al_2O_3\text{-}TiO_x$) inclusions that promote large-scale melt freezing inside the nozzle deposits. Jung *et al.* [6] found that deoxidation by Al addition followed by Ti addition generates clusters Al_2O_3 inclusions, liquid steel thus penetrates though the pores and freezes in the form of patches. Sun *et al.* [7] studied the morphology of oxide inclusions after Al and Ti complex deoxidation. They found that a typical Al-Ti-O inclusion presents a double-layer system with an outer Al_2O_3 layer and an inner TiO_x layer. Doo *et al.* [8] studied the morphology of Al-Ti-O complex oxide inclusions in an ultra low carbon steel melt during the RH process. The morphologies of nearly spherical inclusions containing Ti are quite different from the shape of the alumina inclusions that typically

Corresponding author: De-yong Wang E-mail: wangdy@smm.neu.edu.cn

exhibit a cluster form. In summary, Al-Ti-O inclusions are the main reason for the clogging of submerged nozzles in Ti-bearing Al-killed steel.

The thermodynamic system of Al-Ti-O in molten iron is both indeterminate and incomplete because Ti forms many types of oxides. Some of these oxides have different levels of solid solubility. Moreover, the possible complex oxide phases within the Al-Ti-O system remain unknown. For the Fe-Al-Ti-O system, Ruby-Meyer *et al.* [9] used the multiphase equilibrium code CEQCSI based on the IRSID slag model, and estimated the Fe-Ti-Al-O equilibrium phase diagram at 1793 K. They divided the phase diagram into Al_2O_3, Al_2TiO_5, Ti_2O_3, Ti_3O_5, and an unknown liquid phase. Jung *et al.* [6] employed FACT databases and the FactSage® computing system for determining the oxide phase diagram of the Fe-Al-Ti-O system at 1873 K. However, they did not find a liquid phase. If the liquid inclusions in the Fe-Al-Ti-O system exist, which is made possible by modifying the inclusion composition in this liquid region, the clogging of submerged nozzles will effectively decrease. Unfortunately, no findings on the true composition of liquid inclusions have been published thus far. From the results mentioned above, the formation of liquid inclusions strongly depends on the activity of Al and Ti. Once reoxidation occurs, the equilibrium between the inclusion and molten steel is easily destroyed, and the liquid inclusions may change into harmful solid inclusions. Therefore, for Ti-bearing Al-killed steel, removing or decreasing the TiO_x-Al_2O_3 inclusions from the molten steel is important. In the present work, a typical inclusion of Al_2TiO_5 in an Fe-Al-Ti-O system is synthesized by sintering pure TiO_2 and Al_2O_3 reagents. The inclusions are then immersed into a CaO-SiO_2-Al_2O_3 molten slag for different durations at 1823 K. The dissolution mechanism of the inclusion is discussed by studying the inclusion/slag interface using scanning electron microscopy (SEM) and energy dispersive spectroscopy (EDS).

2. Materials and methods

In the present work, α-type Al_2O_3 (99.999%) and rutile-type TiO_2 (99.999%) were used to prepare the Al_2TiO_5 inclusion. The molar ratio of Al_2O_3 and TiO_2 was 1:1. To increase material consistency, 1.0wt% Y_2O_3 and 1.0wt% SiO_2 were added into the Al_2O_3 and TiO_2 mixture. The powder was thoroughly mixed and impressed into a chip of 2-mm thickness at 50 MPa. The sample was sintered at 1673 K for 150 h under an argon atmosphere. Before and after sintering, the samples were analyzed by X-ray diffraction (XRD; Bruker D8 ADVANCE). The slag was composed of 35wt% CaO, 50wt% SiO_2, and 15wt% Al_2O_3. These compositions roughly represent those of a ladle furnace slag.

The most common method for investigating the dissolution mechanisms of solid oxides in liquid slags and their kinetics is the finger test technique. Here, a refractory material is dipped into a molten slag and exposed for a certain period of time. In the present study, the prepared Al_2TiO_5 inclusion was immersed into a CaO-SiO_2-Al_2O_3 molten slag. The dissolution experiments were carried out in platinum crucibles with a dimension of ϕ30 mm×50 mm. About 10 g of slag powder was placed into the crucible and heated to 1823 K under an argon atmosphere in an electric resistance furnace. The temperature was held constant for 10 min for homogeneous slag melting. The inclusion sample was then strapped to a small slot at the end of an alumina bar. The samples were stopped above the liquid slag surface for 2 min, and then dipped into the slag. After the dissolution time of 0, 10, 30, and 60 s, samples were taken out immediately and cooled to room temperature under argon airflow. Then, the section between the slag and inclusion was cut and polished. SEM and EDS were conducted to observe the microscopic structure of the reaction interface, and to determine composition changes in the reactant elements.

3. Results and discussion

Fig. 1 shows the variations in the XRD charts of the samples before and after sintering. The new Al_2TiO_5 phase forms after sintering for 150 h at 1673 K. Because Al_2TiO_5 is formed by the solid phase diffusivity between Al_2O_3 and TiO_2, wherein an incomplete reaction is easily induced, several unreacted Al_2O_3 and TiO_2 molecules remain in the mixture. The Al_2TiO_5 content in the sample is approximately 90% based on semiquantitative XRD determination.

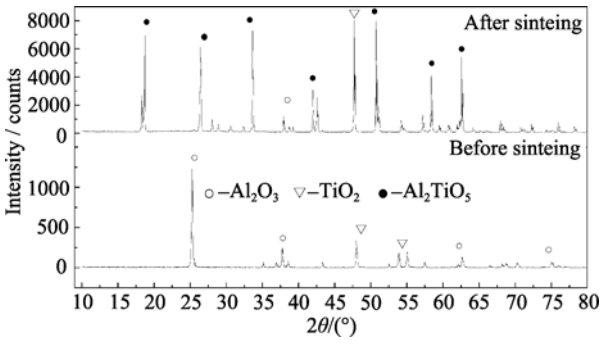

Fig. 1. XRD chart of the samples before and after sintering at 1673 K.

3.1. Characteristics of the dissolution boundary

Fig. 2 shows a typical SEM image of the dissolution boundary between the inclusion and slag with reaction time of 10 s. It shows that the bulk slag is denser than the inclusion body, and a clear mark between the inclusion and slag can be observed. However, the mark shifts to different places at different reaction time. Therefore, along the boundary between the inclusion and bulk slag, the composition change from the line scanning method by EDS reveals the dissolution process of the inclusion. The composition determined by EDS for different points in Fig. 2 is listed in Table 1. Points 1 and 2 represent the inclusion body, and points 5-7 lie in the liquid slag region. Thus, the distance from points 3 to 4 is proposed as the dissolution boundary because of the rapid decrease in Ti and Al, as well as the increase in Si and Ca. This proves that inclusion dissolution and slag penetration simultaneously occur. For the composition of points 5-7, the $w(CaO)/w(SiO_2)$ values of the slag near the slag/inclusion boundary are slightly lower than that of the original bulk slag ($w(CaO)/w(SiO_2)$=0.7). This indicates that the diffusion or penetration rate of SiO_2 toward the inclusion is faster than that of CaO. Similar results were reported by Oishi [10], Cho [11], and Park [12-13] for Al_2O_3 dissolution reactions in the CaO-Al_2O_3-SiO_2 slag.

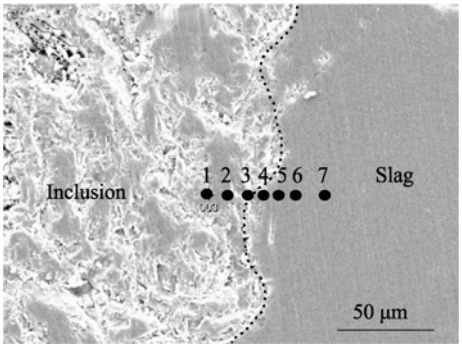

Fig. 2. SEM image of the inclusion/slag interface with the dissolution time of 10 s.

Table 1. Composition at different points in Fig. 2 wt%

Point	Al_2O_3	SiO_2	CaO	TiO_x
1	53.28	0.6	0.00	46.12
2	50.75	1.79	0.00	47.46
3	37.19	19.06	17.06	26.69
4	15.3	41.8	30.56	12.34
5	7.41	68.47	22.94	1.17
6	7.47	60.95	31.13	0.46
7	7.21	60.16	32.48	0.15

3.2. Dissolution mechanism of the Al_2TiO_5 inclusions in the molten slag

Fig. 3 summarizes the dissolution boundary variations with reaction time and shows that the boundary thickness increases with reaction time. At 0 s, the inclusion is just immersed into the molten slag and then taken out immediately. In this case, the boundary thickness is about 6 μm. As the reaction time increases, the dissolution boundary thickness increases to 50, 80, and 75 μm at 10, 30, and 60 s, respectively. Thus, the dissolution rate of the inclusion is not constant. The dissolution rate is initially high and then gradually decreases. In many studies, researchers believe that the dissolution rate of materials in molten slags or steel is controlled by the diffusion of solute elements and not by the chemical reaction. The present dissolution process of Al_2TiO_5 in the slag is in agreement with that observed in previous studies. Moreover, the Ti and Al concentrations often fluctuate widely between the inclusion and bulk slag. Table 2 lists the composition at different points in the SEM images at different reaction time. At 10 s, the line scanning results show that there are two separate dissolution boundaries (from points 3 to 4, as well as points 6 to 10). In this case, there are two boundaries near the reaction region, the dissolution path can be broken by another remaining inclusion due to the liquid slag permeation, therefore, the slag permeation toward the inclusion is proved by these experimental results.

In many cases, a solid oxide layer and an inner liquid phase product around the solid inclusion can be observed during inclusion dissolution in a slag. Sandhage and Yurek [14] previously studied the dissolution process of Al_2O_3 in the CaO-SiO_2-Al_2O_3-MgO slag at 1723 and 1823 K. The results of electron probe microanalysis (EPMA) confirmed that the inner liquid product corresponds to the liquid composition co-saturated with Al_2O_3 and $MgAl_2O_4$. Park *et al.* [12] and Valdez *et al.* [15], using the confocal scanning laser microscopy (CSLM) technique, found that $MgAl_2O_4$ has a ring-like structure for the dissolution of the MgO inclusion in the CaO-SiO_2-Al_2O_3-MgO slag at 1773 K. However, the formation mechanism of the solid phase products ($MgAl_2O_4$ or Ca_2SiO_4) is difficult to explain with the CSLM results. In the present work, the solid oxide layer around the inclusion was not observed according to the experimental data. The compositions at different points in the SEM images (analyzed by SEM-EDS) in Table 2 all indicate that the compound CaO-SiO_2-Al_2O_3-TiO_x is a type of reaction product during the dissolution of Al_2TiO_5 in the slag. The dissolution product is typically composed of a $w(CaO)/w(SiO_2)$ value of

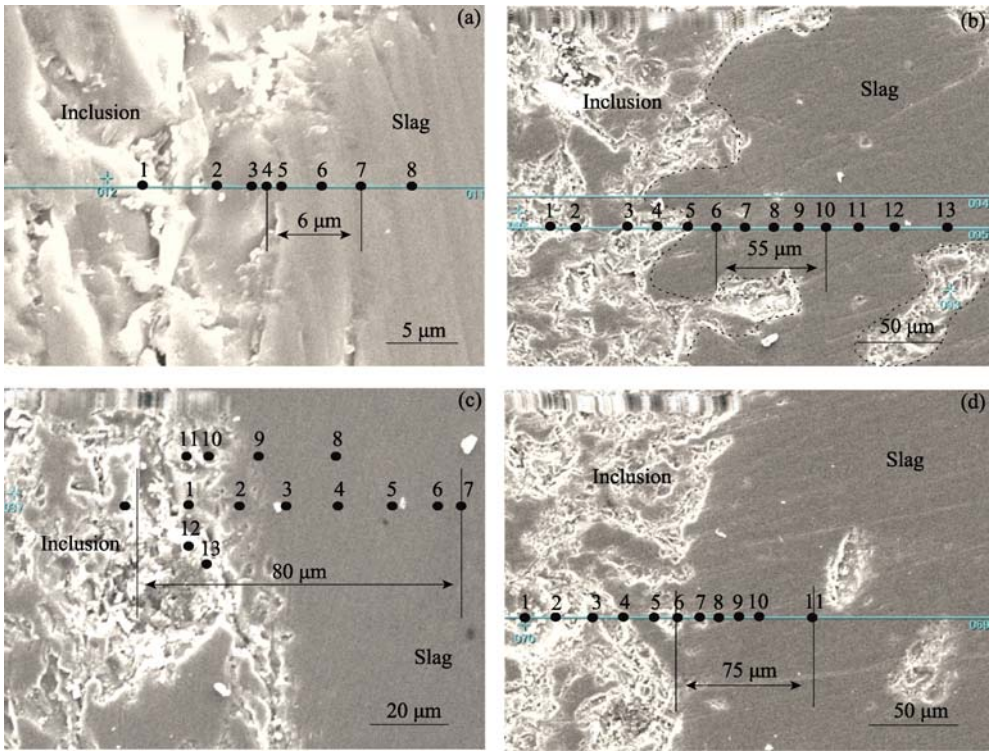

Fig. 3. Variations of the dissolution boundary at different reaction time: (a) 0 s; (b) 10 s; (c) 30 s; (d) 60 s.

Table 2. Composition at different points in SEM images at different reaction time **wt%**

Reaction time / s	Point	Al_2O_3	SiO_2	CaO	TiO_x
0	1	57.20	1.27	0.73	40.80
	2	55.69	2.41	1.22	40.68
	3	54.33	1.20	3.04	41.43
	4	53.33	2.03	1.68	42.96
	5	22.67	39.35	22.94	15.04
	6	18.90	42.76	32.86	5.48
	7	12.48	55.99	28.88	2.65
	8	9.35	61.86	27.76	1.03
10	1	55.41	7.37	3.18	34.04
	2	49.11	4.51	1.08	45.29
	3	20.22	42.50	27.76	9.52
	4	21.03	27.06	33.33	18.58
	5	55.27	2.31	2.23	40.19
	6	51.02	2.15	0.38	46.45
	7	21.43	30.97	32.67	14.94
	8	16.43	38.94	31.96	12.67
	9	16.75	45.78	32.72	4.75
	10	14.71	52.76	28.35	4.18
	11	11.73	57.99	28.59	1.69
	12	8.48	61.96	28.98	0.58

0.7-1.2, 15wt%-20wt% Al_2O_3, and 5wt%-15wt% TiO_x. Incidentally, the dissolution process of the inclusion may induce the oxidation-reduction reaction for Ti, and the total oxide of titanium is only considered as TiO_2. To confirm that the dissolution product is a liquid phase, FactSage® software was used to calculate the liquid surface of the Al_2O_3-CaO-SiO_2-TiO_2 phase diagram with 15wt% Al_2O_3 as shown in Fig. 4. The composition of the dissolution product at the slag/inclusion boundary from the EDS analysis (Table 2) is then simplified and marked using black solid points shown in Fig. 4. The composition of the typical dissolution product is found to be in the range of 1673-1773 K, confirming that it may be liquid phase under steelmaking conditions.

Based on present and previous results, a feasible dissolution mechanism of the Al_2TiO_5 inclusion in a CaO-SiO_2-Al_2O_3 slag is proposed. During the initial stage, the liquid phase dissolution product (Al_2O_3-CaO-SiO_2-TiO_2) forms on the inclusion surface, against which the dissolution boundary begins to appear. After this stage, the thickness of the dissolution boundary slowly increases because the dissolution rate of the Al_2TiO_5 inclusion is faster than the diffusion rate of the liquid product toward the bulk slag. With increasing reaction time, the boundary reaches the

largest distance, the dissolution rate of Al_2TiO_5 equals the diffusion rate of the liquid product, and the dissolution process remains stable until the inclusion is completely dissolved. These dissolution behaviors appear to satisfy the features of the shrinking core model with the existence of the reaction product layer. Because the diffusion rate of the liquid phase is the rate-determining step, raising the temperature and optimizing the slag composition are keys for improving the dissolution rate of the inclusion. These issues will be studied in a future research.

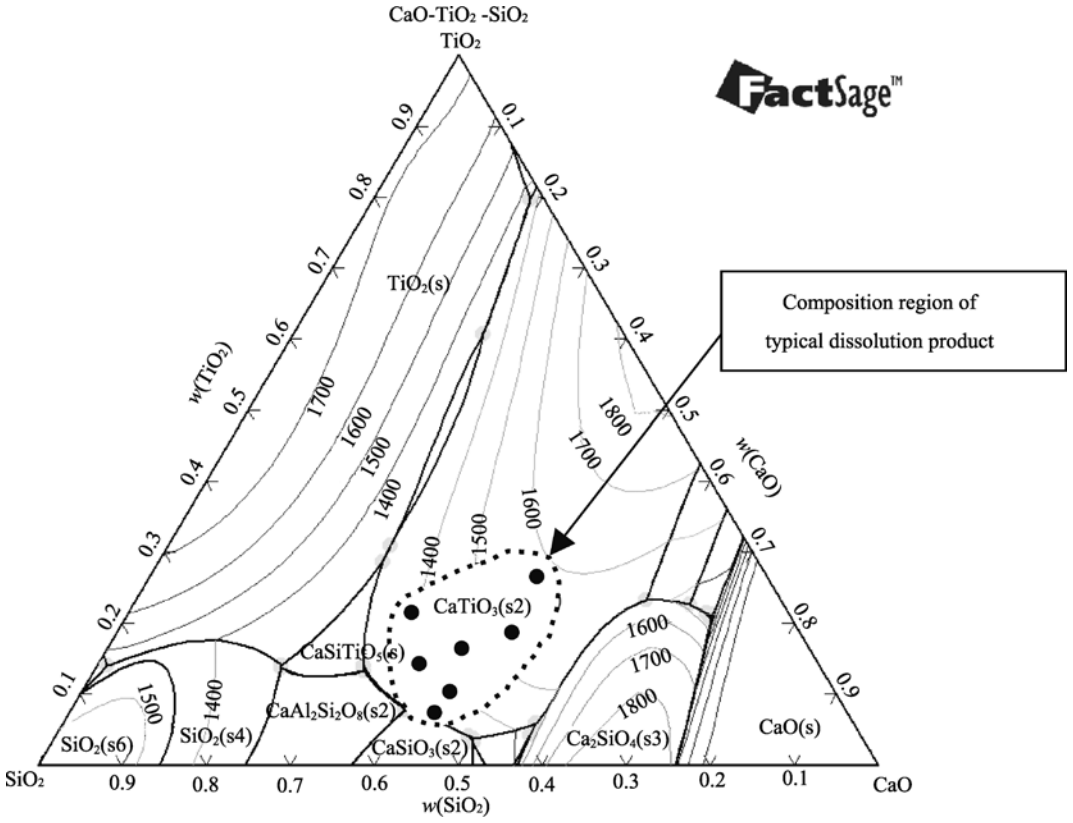

Fig. 4. Liquid surface and typical composition of dissolution products in the $CaO\text{-}SiO_2\text{-}TiO_2$ system.

4. Conclusions

(1) Al_2TiO_5 inclusions were prepared by sintering an Al_2O_3 and TiO_2 mixture for 150 h at 1673 K. The inclusion samples had good densities, which benefit the dissolution of inclusions in the molten slag.

(2) The decrease in Ti and Al, and the increase in Si and Ca in the dissolution boundary prove that inclusion dissolution and slag penetration simultaneously occur.

(3) When the Al_2TiO_5 sample is dissolved in the slag, a liquid product forms on the surface of the inclusion, against which the dissolution boundary begins to appear. The liquid product is composed of a $w(CaO)/w(SiO_2)$ value of 0.7-1.2, 15wt%-20wt% Al_2O_3, and 5wt%-15wt% TiO_x. Initially, the dissolution rate of the Al_2TiO_5 inclusion is faster than the diffusion rate of the liquid product toward the bulk slag. With increasing reaction time, the boundary reaches the largest distance, the dissolution rate of Al_2TiO_5 equals the diffusion rate of the liquid product in the bulk slag, and the dissolution process remains stable until the inclusion is completely dissolved.

References

[1] K. Yamamoto, T. Hasegawa, and J. Takamura, Effect of boron on intra-granular ferrite formation in Ti-oxide bearing steels, *ISIJ Int.*, 36(1996), No.1, p.80.

[2] L.M. Peng, Z. Li, and H. Li, Effects of microalloying and ceramic particulates on mechanical properties of TiAl-based alloys, *J. Mater. Sci.*, 41(2006), No.22, p.7524.

[3] M. Vedani and A. Mannucci, Effect of titanium addition on precipitate and microstructural control in C-Mn microalloyed steel, *ISIJ Int.*, 42(2002), No.12, p.1520

[4] Y. Kawashima, Y. Nagata, and K. Shinme, Influence of Ti concentration on nozzle clogging on Al-Ti deoxidation: be-

havior of inclusion on Al-Ti deoxidation-2, *CAMP-ISIJ*, 4(1991), No.4, p.1237.

[5] S. Basu, S.K. Choudhary, and N.U. Girase, Nozzle clogging behaviour of Ti-bearing Al-killed ultra low carbon steel, *ISIJ Int.*, 44(2004), No.10, p.1653.

[6] I.H. Jung, S.A. Decterov, and A.D. Pelton, A thermodynamic model for deoxidation equilibrium in steel, *Metall. Mater. Trans. B*, 35(2004), No.3, p.493.

[7] M.K. Sun, I.H. Jung, and H.G. Lee, Morphology and chemistry of oxide inclusions after Al and Ti complex deoxidation, *Met. Mater. Int.*, 14(2008), No.6, p.791.

[8] W.C. Doo, D.Y. Kim, S.C. Kang, *et al*., The morphology of Al-Ti-O complex oxide inclusions formed in an ultra low-carbon steel melt during the RH process, *Met. Mater. Int.*, 13(2007), No.3, p.249.

[9] F. Ruby-Meyer, J. Lehmann, and H. Gaye, Thermodynamic analysis of inclusion in Ti-deoxidized steel, *Scand. J. Metall.*, 29(2000), No.5, p.206.

[10] Y. Oishi, A.R. Cooper Jr., and W.D. Kingery, Dissolution in ceramic systems: III. Boundary layer concentration gradients, *J. Am. Ceram. Soc.*, 48(1965), No.2, p.88.

[11] W.D. Cho and P. Fan, Diffusional dissolution of alumina in various steelmaking slag, *ISIJ Int.*, 44(2004), No.2, p.229.

[12] J.H. Park, I.H. Jung, and H.G. Lee, Dissolution behavior of Al_2O_3 and MgO inclusions in the $CaO-Al_2O_3-SiO_2$ slag: formation of ring-like structure of $MgAl_2O_4$ and Ca_2SiO_4 around MgO inclusions, *ISIJ Int.*, 46(2006), No.11, p.1626.

[13] J.J. Park, J.O. Jo, S.I. Kim, *et al.*, Thermodynamics of titanium and oxygen dissolved in liquid iron equilibrated with titanium oxides, *ISIJ Int.*, 47(2007), No.1, p.16.

[14] K.H. Sandhage and G.J. Yurek, Indirect dissolution of sapphire into silicate melts, *J. Am. Ceram. Soc.*, 71(1998), No.6, p.478.

[15] M. Valdez, G.S. Shannon, and S. Sridhar, The ability of slags to absorb Solid oxide inclusions, *ISIJ Int.*, 46(2006), No.3, p.450.